Robust Lyapunov-Based Feedback Control of Nonlinear Web-Winding Systems[†]

Matthew D. Baumgart and Lucy Y. Pao
Electrical and Computer Engineering Department
University of Colorado
Boulder, CO 80309-0425
baumgarm@colorado.edu and pao@colorado.edu

***Abstract*— Web-winding systems such as tape drives are often modeled as linear and time-invariant (LTI), but at least two nonlinearities are common in these systems. First, the reel radii and moments of inertia change as web media spools from one reel to another. Second, friction can draw a thin layer of air between the layers of web media wrapped on the takeup reel, making the system's spring and damping characteristics nonlinear by allowing a greater length of media to vibrate freely. Little has been published regarding the dynamic behavior of this "air entrainment" phenomenon. This paper first describes a model for web-winding systems that includes these nonlinearities. No particular model is taken for air entrainment; it is only assumed that its effects are bounded in a certain sense. It is further assumed that the motor parameters are not known exactly. Feedback linearization, state feedback, and changes of variables are then used to transform the system into decoupled and intuitively meaningful tension and velocity loops. Lyapunov redesign techniques are then used to develop control laws that are robust with respect to the motor parameters. Under these laws, velocity error is exponentially stable and tension error satisfies a desired bound for all time—with tension error also exponentially stable in the steady-state case. Simulations illustrate the performance of these schemes.**

I. Introduction

Reel-to-reel web-winding systems are common in the fabrication and transport of materials such as paper, metal, and photographic film. They are integral to information storage systems using magnetic tape, and also have applications in entertainment. Advances in web-winding system control may improve transient performance, reliability, and tracking of the desired web velocity and tension. A more robust control scheme may also reduce costs by diminishing the need for lengthy and costly "tuning" of controllers or expensive, tightly specified hardware components. This paper develops such schemes largely from the perspective of tape systems.

A basic model for web-winding systems is linear and time invariant (LTI) [2]. However, a number of nonlinearities and disturbances affect the system. First, the radii and moments of inertia of the two reels slowly vary as tape spools from one reel to the other. Second, a nonlinear effect called "air entrainment" occurs when friction draws a thin layer of air many layers deep into the pack of web media wrapped on the takeup reel. This allows a greater length of the media to vibrate, effectively making the spring and damping parameters time-varying. Little has been published about the dynamics of air entrainment, though some work has been done investigating the steady-state phenomenon [3], [8].

Another complication stems from the use of DC-motors to drive the reels. In practice, the constants characterizing these motors are only specified within a certain range, with more tightly specified motors costing more. This uncertainty is often ignored in the literature, but it may be important if motor costs are an issue. Section II presents a nonlinear web-winding model that extends the model of [7] to include these uncertainties and nonlinearities.

Several control schemes have been presented in the literature. A "textbook" control system is described in [2], which addresses only the LTI system model and does not account for changing reel radii, air entrainment, or any other disturbances. Another technique applies sequential loop closing [7]. Other gain-scheduled or H_∞ controllers form the bulk of the tape system control literature [5], [6], [9]. In [5], [6], [7], a disturbance observer is used with success to reduce the effects of reel eccentricity and stiction. Further, some of these controllers are gain-scheduled over the steady-state values of air entrainment at each velocity.

These schemes are shown to be stable at various steady-state operating points. However, if reel velocities change (say, from zero to operating velocity) then air entrainment changes the spring and damping parameters *during the maneuver*. In this case the system is not in "steady-state." The stability of existing controllers has yet to be established analytically for the whole nonlinear system (i.e., where entrained air and the reel radii and moments are dynamical variables). Further, gain-scheduled linear controllers have the potential disadvantage of being costly and time-consuming to tune [6]. The H_∞ designs may also be of high order. Finally, none of these schemes addresses the inevitable motor parameter uncertainties. While these schemes have proven workable in practice, a nonlinear control strategy may offer advantages in clarity, performance, and the tractability of stability analysis. It may also help reduce hardware and development costs.

This paper presents a robust nonlinear feedback controller that is robust to uncertainties in the motor torque and friction parameters, and treats air entrainment as a dynamical variable. No particular model is assumed for air entrainment;

[†]This work was supported in part by the Colorado Center for Information Storage and the National Science Foundation (Grant CMS–0201459).

rather, the spring and damping parameters are taken to be wholly unknown and time-varying with the assumption that they satisfy reasonable bounds. The controller is robust over all such parameter trajectories. Like existing schemes, it assumes that measurements of tension and reel velocity measurements are always available. It also requires knowledge of the reel radii and moments, which are available in practice by using the reel velocity measurements to keep track of how much web media is on each reel.

To develop the controller, the nonlinear system model is first manipulated in Section III via feedback linearization and changes of variables. Linear state feedback is also added, with the gains left undetermined. The resulting equations are intuitively useful in that, except for disturbance terms that account for possible modeling errors, the tension and velocity loops are independent and linear.

Control laws are developed in Section IV. It is well known that feedback linearization is sensitive to modeling errors, and the model here contains four motor constants that may be known only within a specified range. Lyapunov redesign [4] is applied to make the feedback control robust to these uncertainties. This redesign is interesting because it is applied to each loop separately and does not require knowledge of the air entrainment effects on the system. It is shown that the feedback gains can be chosen so that:

- the velocity error goes to zero exponentially fast, where the time constant can be chosen arbitrarily (subject only to actuator limitation constraints);
- the tension error stays in a desired range for all time;
- the tension error goes to zero exponentially fast in steady-state (i.e., when air entrainment is constant).

The development of this baseline controller emphasizes intuitive clarity and simplicity. To both improve transient response and reduce peak motor currents, a modified saturating controller is also developed for the velocity loop. Simulations in Section V show the performance of both the baseline and modified controllers under various air entrainment scenarios, with modeling errors introduced as well.

Note: Some controls discussed are discontinuous, and hence it is not immediately clear that state trajectories exist for the associated discontinuous differential system equations. This is not necessarily a practical concern, in part because in implementation one would apply a continuous approximation to the sign$\{\cdot\}$ function, and also because states of a real web-winding system must always exist. In any case, the results in this paper show that *if state trajectories exist* then they have certain stability or boundedness properties.

II. Nonlinear Web-Winding System Model

This section reviews system equations for a web-winding system, building on the development in [7]. Air entrainment and motor parameter uncertainties are also formulated.

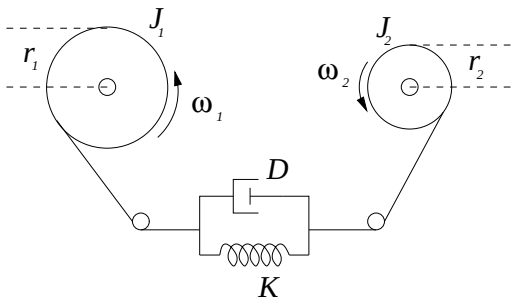

Fig. 1. Linear model for web-winding system.

A. System Equations

Figure 1 shows the well-known lumped-parameter model for web transport. The reels have radii $r_1(t)$ and $r_2(t)$, moments of inertia $J_1(t)$ and $J_2(t)$, and turn with angular velocities $\omega_1(t)$ and $\omega_2(t)$. The length of web media between the reels has tension $T(t)$, and is modeled by a spring and dashpot with time-varying parameters $K(t)$ and $D(t)$, in parallel. DC motors driven by currents $u_1(t)$ and $u_2(t)$ turn the reels. The reel moments are related to the radii by

$$J_{1,2}(t) = J_m + K_J(r_{1,2}^4 - r_I^4) \tag{1}$$

where J_m is the moment of inertia of an empty reel and motor, r_I is the radius of an empty reel, and $K_J = t_p t_w \pi/2$, where t_p and t_w denote tape density and width, respectively. The radii and moments of inertia vary according to

$$\begin{aligned} \dot{r}_1(t) &= -\frac{\epsilon\omega_1(t)}{2\pi}, \\ \dot{r}_2(t) &= \frac{\epsilon\omega_2(t)}{2\pi}, \\ \dot{J}_1(t) &= -\frac{2K_J\epsilon\omega_1(t)r_1^3(t)}{\pi}, \\ \dot{J}_2(t) &= \frac{2K_J\epsilon\omega_2(t)r_2^3(t)}{\pi}, \end{aligned} \tag{2}$$

where ϵ denotes tape thickness. It is convenient to express the state of the system in terms of the reel/moment vector $\mathbf{y}(t) \equiv [r_1(t) \;\; r_2(t) \;\; J_1(t) \;\; J_2(t)]^\top$, the tension $T(t)$, and the tangential reel velocities

$$\begin{aligned} V_1(t) &= r_1(t)\omega_1(t), \\ V_2(t) &= r_2(t)\omega_2(t), \end{aligned} \tag{3}$$

where $^\top$ denotes transpose. The tape velocity is defined as $V(t) \equiv (V_1(t) + V_2(t))/2$. Using equations (2) and substituting $K(t) = \sigma D(t)$ as explained below in Subsection II-B, the state equations can now be derived via Newtonian dynamics as in [7], with the difference that $D(t)$ and $K(t)$ are not constants. The resulting state equations are (2) and

$$\dot{\mathbf{x}} = \mathbf{A}(\mathbf{y}, D)\mathbf{x} + \mathbf{B}(\mathbf{y}, D)\mathbf{u} + \frac{\epsilon}{2\pi}\mathbf{d}(\mathbf{x}, \mathbf{y}, D), \tag{4}$$

with

$$\begin{aligned}\mathbf{x}(t) &\equiv [T(t)\ \ V_1(t)\ \ V_2(t)]^\top,\\ \mathbf{u}(t) &\equiv [u_1(t)\ \ u_2(t)]^\top,\end{aligned}$$

and

$$\mathbf{A}(\mathbf{y},D) \equiv \begin{bmatrix} \frac{\dot{D}(t)}{D(t)} - D(t)\left(\frac{r_1^2(t)}{J_1(t)} + \frac{r_2^2(t)}{J_2(t)}\right) & D(t)\left(\frac{\beta_1}{J_1(t)} - \sigma\right) & D(t)\left(\sigma - \frac{\beta_2}{J_2(t)}\right)\\ r_1^2(t)/J_1(t) & -\beta_1/J_1(t) & 0\\ -r_2^2(t)/J_2(t) & 0 & -\beta_2/J_2(t)\end{bmatrix},$$

$$\mathbf{B}(\mathbf{y},D) \equiv \begin{bmatrix} -\frac{D(t)r_1(t)K_{t1}}{J_1(t)} & \frac{D(t)r_2(t)K_{t2}}{J_2(t)}\\ \frac{r_1(t)K_{t1}}{J_1(t)} & 0\\ 0 & \frac{r_2(t)K_{t2}}{J_2(t)}\end{bmatrix},$$

$$\mathbf{d}(\mathbf{x},\mathbf{y},D) \equiv \begin{bmatrix} D(t)\left(\frac{V_1^2(t)}{r_1^2(t)}\left(1 - \frac{4K_J r_1^4(t)}{J_1(t)}\right) + \frac{V_2^2(t)}{r_2^2(t)}\left(1 - \frac{4K_J r_2^4(t)}{J_2(t)}\right)\right)\\ -\frac{V_1^2(t)}{r_1^2(t)}\left(1 - \frac{4K_J r_1^4(t)}{J_1(t)}\right)\\ \frac{V_2^2(t)}{r_2^2(t)}\left(1 - \frac{4K_J r_2^4(t)}{J_2(t)}\right)\end{bmatrix},$$

where K_{t1} and β_1 denote the torque and friction constants of motor 1, and similarly for motor 2. The term in $\mathbf{d}(\mathbf{x},\mathbf{y},D)$ is due to the slowly-varying reel radii and moments of inertia. For many systems ϵ is so small that this term can be ignored, but it is retained here since it adds only trivial complications.

B. Air Entrainment

Air entrainment in the takeup reel changes the length of web media that is free to vibrate, which is called the "unsupported tape length" $L(t)$ in tape systems [8]. This leads to nonlinearities because according to structural mechanics the spring and damping parameters vary inversely with $L(t)$:

$$K(t) = \frac{c_K}{L(t)}, \quad D(t) = \frac{c_D}{L(t)}, \tag{5}$$

where c_K and c_D are constants of the web media. These expressions are readily derived by considering a chain of linear springs (or dashpots) connected in series. Expressing $K(t)$ in terms of $D(t)$ by

$$K(t) = \sigma D(t), \tag{6}$$

where $\sigma = c_K/c_D$, simplifies the model. In fact, the results of this paper do not require (5) to hold, but just that (6) holds for some constant σ.

The literature includes few dynamic models for $L(t)$, though [1] proposes a simple model. No specific model is used in this paper. Rather, it is simply assumed that $L(t)$ and its derivative are bounded above and below (and the lower bound on $L(t)$ is of course positive). Then $D(\cdot) \in \mathcal{D}$, with

$$\mathcal{D} \equiv \left\{ f(t) \in \mathcal{C}^1 \;\middle|\; \begin{array}{c} D_{min} \le f(t) \le D_{max}, \forall t\\ |\dot{f}(t)| \le \dot{D}_{max}, \forall t\end{array} \right\}, \tag{7}$$

where $\mathcal{C}^1$ denotes the continuously differentiable functions and D_{min}, D_{max}, and $\dot{D}_{max}$ are positive constants. These constants might be determined by experiments similar to [3] or modeling approaches like [3], [8]. In this paper $D(\cdot) \in \mathcal{D}$ is considered an unknown and time-varying parameter.

C. Parameter Uncertainties

In practice the motor constants K_{ti} and β_i, where $i \in \{1,2\}$, are usually specified only within given ranges:

$$K_{ti} \in [K_{ti_{min}}, K_{ti_{max}}], \quad \beta_i \in [\beta_{i_{min}}, \beta_{i_{max}}]. \tag{8}$$

The size of these ranges varies inversely with motor cost. Controllers must be implemented using estimates (or "nominal values") $\hat{K}_{ti}$ and $\hat{\beta}_i$ of these constants.

III. Transformation of the Model

In this section the model is manipulated via three intuitive steps, resulting in separate tension and velocity loops. For the algebra these steps require, it is often helpful to note that the matrix $\mathbf{B}(\mathbf{y},D)$ in (4) can be factored as

$$\mathbf{B}(\mathbf{y},D) = \begin{bmatrix} -D(t) & D(t)\\ 1 & 0\\ 0 & 1\end{bmatrix} \mathbf{N}^{-1}(\mathbf{y}), \tag{9}$$

where

$$\mathbf{N}(\mathbf{y}) \equiv \begin{bmatrix} \frac{J_1(t)}{r_1(t)K_{t1}} & 0\\ 0 & \frac{J_2(t)}{r_2(t)K_{t2}}\end{bmatrix}.$$

Time-dependence is suppressed in some expressions below.

A. Shifting to an Error System

First, the model described by (2) and (4) is transformed by a change of variables and input shift into an error system about a desired setpoint $\mathbf{x}_d \equiv [T_d\ \ V_d\ \ V_d]^\top$. Define the error states $\mathbf{e}_x(t) = [e_T(t)\ \ e_1(t)\ \ e_2(t)]^\top \equiv \mathbf{x}(t) - \mathbf{x}_d$ and let

$$\mathbf{u}(t) = \hat{\mathbf{N}}(\mathbf{y})\hat{\mathbf{u}}_0(t) + \mathbf{u}_a(t), \tag{10}$$

where

$$\hat{\mathbf{u}}_0(t) \equiv \begin{bmatrix} \frac{-r_1^2(t)T_d}{J_1(t)} + \frac{\hat{\beta}_1 V_d}{J_1(t)} + \frac{\epsilon V_1^2(t)}{2\pi r_1^2(t)}\left(1 - \frac{4K_J r_1^4(t)}{J_1(t)}\right)\\ \frac{r_2^2(t)T_d}{J_2(t)} + \frac{\hat{\beta}_2 V_d}{J_2(t)} - \frac{\epsilon V_2^2(t)}{2\pi r_2^2(t)}\left(1 - \frac{4K_J r_2^4(t)}{J_2(t)}\right)\end{bmatrix}$$

$$\hat{\mathbf{N}}(\mathbf{y}) \equiv \begin{bmatrix} \frac{J_1(t)}{r_1(t)\hat{K}_{t1}} & 0\\ 0 & \frac{J_2(t)}{r_2(t)\hat{K}_{t2}}\end{bmatrix}.$$

The term $\mathbf{u}_a(t)$ is determined below. The term $\hat{\mathbf{N}}(\mathbf{y})\hat{\mathbf{u}}_0(t)$ attempts to cancel $\mathbf{d}(\mathbf{x},\mathbf{y},D)$ and the terms in T_d and V_d that appear when one makes the change of variables $\mathbf{x}(t) = \mathbf{x}_d + \mathbf{e}_x(t)$ in (4). The system equations then become (2) and

$$\dot{\mathbf{e}}_x = \mathbf{A}(\mathbf{y},D)\mathbf{e}_x + \mathbf{B}(\mathbf{y},D)\left(\mathbf{u}_a - \Delta_e\right) + \begin{bmatrix} \frac{\dot{D}(t)T_d}{D(t)}\\ 0\\ 0\end{bmatrix}, \tag{11}$$

where

$$\Delta_e(t) = \tilde{\mathbf{N}}(\mathbf{y})\hat{\mathbf{u}}_0(t) + \mathbf{N}(\mathbf{y})V_d \begin{bmatrix} \frac{\tilde{\beta}_1}{J_1(t)} \\ \frac{\tilde{\beta}_2}{J_2(t)} \end{bmatrix}$$

with $\tilde{\mathbf{N}}(\mathbf{y}) \equiv \mathbf{N}(\mathbf{y}) - \hat{\mathbf{N}}(\mathbf{y})$ and $\tilde{\beta}_i \equiv \beta_i - \hat{\beta}_i$. The error term Δ_e arises since motor parameter uncertainty causes imperfect cancellation. Note that if $\tilde{K}_{ti} \equiv K_{ti} - \hat{K}_{ti} = 0$ and $\tilde{\beta}_i = 0$ then $\Delta_e = 0$. The disturbance term $\dot{D}(t)T_d/D(t)$ (caused by air entrainment) cannot be cancelled. Without this disturbance and the term Δ_e, the system (11) would have an equilibrium point at the origin for $\mathbf{u}_a = 0$.

B. Feedback linearization

Feedback is now used to linearize the system and obviate the need for (2) to be considered as part of the system equations. State feedback is also added for the purposes of control, with feedback coefficients left undetermined at present. Taking advantage of knowledge of $\mathbf{y}(t)$, let

$$\mathbf{u}_a(t) = \hat{\mathbf{N}}(\mathbf{y})\hat{\mathbf{M}}(\mathbf{y})\mathbf{e}_x(t) + \hat{\mathbf{N}}(\mathbf{y})\mathbf{R}\mathbf{u}_b(t), \tag{12}$$

where $\mathbf{u}_b(t) = [u_{b1}(t) \;\; u_{b2}(t)]^\top$ is determined below and

$$\hat{\mathbf{M}}(\mathbf{y}) \equiv \begin{bmatrix} -p - \frac{r_1^2(t)}{J_1(t)} & s + \frac{\hat{\beta}_1}{J_1(t)} & c \\ p + \frac{r_2^2(t)}{J_2(t)} & c & s + \frac{\hat{\beta}_2}{J_2(t)} \end{bmatrix},$$

$$\mathbf{R} \equiv \begin{bmatrix} 1 & -1 \\ 1 & 1 \end{bmatrix},$$

for some gains $p, s,$ and c. The second term on the right-hand side of (12) helps decouple the tension and velocity loops below, where $\mathbf{R}$ is a decoupling matrix. The first term provides state feedback. Symmetry motivates the choice to parameterize $\hat{\mathbf{M}}(\mathbf{y})$ with just three distinct feedback gains instead of six. For instance, one intuitively expects that the gain from a reel's velocity to its input current should be the same for both reels. The gains c and s represent "self" and "cross" feedback, while the reels get opposite tension feedback $\pm p$ because tension provides them opposite torques. The "extra" terms in $\hat{\mathbf{M}}(\mathbf{y})$ with $J_i(t)$ in the denominator provide feedback linearization by cancelling terms in $\mathbf{A}(\mathbf{y}, D)$. This cancellation is imperfect if $\hat{\beta}_i \neq \beta_i$. The matrix $\hat{\mathbf{N}}(\mathbf{y})$ in (12) attempts to cancel $\mathbf{N}^{-1}(\mathbf{y})$ in (9), which causes additional errors if $\hat{K}_{ti} \neq K_{ti}$. The state equations are now

$$\dot{\mathbf{e}}_x = \begin{bmatrix} 2D(t)p & D(t)(c-s-\sigma) & -D(t)(c-s-\sigma) \\ -p & s & c \\ p & c & s \end{bmatrix} \mathbf{e}_x + \begin{bmatrix} \frac{\dot{D}(t)}{D(t)}(T_d + e_T(t)) \\ 0 \\ 0 \end{bmatrix} + \mathbf{B}(\mathbf{y}, D)\left(\hat{\mathbf{N}}(\mathbf{y})\mathbf{R}\mathbf{u}_b - \Delta\right), \tag{13}$$

where

$$\Delta(t) = \tilde{\mathbf{N}}(\mathbf{y})\left(\hat{\mathbf{u}}_0(t) + \hat{\mathbf{M}}(\mathbf{y})\mathbf{e}_x(t)\right) + \mathbf{N}(\mathbf{y}) \begin{bmatrix} \frac{\tilde{\beta}_1 V_1(t)}{J_1(t)} \\ \frac{\tilde{\beta}_2 V_2(t)}{J_2(t)} \end{bmatrix}.$$

Note that the system matrix is now independent of $\mathbf{y}(t)$, and linear if $D(\cdot)$ is considered a time-varying parameter.

C. Decoupling Transformation

Making use of (9), the state transformation

$$\begin{aligned} e_V(t) &\equiv \frac{e_1(t) + e_2(t)}{2} = V(t) - V_d, \\ e_W(t) &\equiv \frac{e_1(t) - e_2(t)}{2}, \end{aligned} \tag{14}$$

yields an intuitively attractive set of system equations:

$$\begin{bmatrix} \dot{e}_T \\ \dot{e}_W \\ \dot{e}_V \end{bmatrix} = \mathbf{F}(D) \begin{bmatrix} e_T \\ e_W \\ e_V \end{bmatrix} + \begin{bmatrix} \frac{\dot{D}}{D}(T_d + e_T) \\ 0 \\ 0 \end{bmatrix} + \mathbf{G}(D)\Big[\mathbf{u}_b - \mathbf{R}^{-1}\mathbf{N}^{-1}(\mathbf{y})\Big(\tilde{\mathbf{N}}(\mathbf{y})\mathbf{R}\mathbf{u}_b + \Delta\Big)\Big], \tag{15}$$

where

$$\mathbf{F}(D) = \begin{bmatrix} 2D(t)p & 2D(t)(c-s-\sigma) & 0 \\ -p & s-c & 0 \\ 0 & 0 & s+c \end{bmatrix},$$

$$\mathbf{G}(D) = \begin{bmatrix} 0 & 2D(t) \\ 0 & -1 \\ 1 & 0 \end{bmatrix}.$$

Error terms due to motor parameter uncertainties in the equilibrium shift, feedback linearization, and decoupling enter the equation at the same point as $\mathbf{u}_b$. Note that the "tension loop" (in e_T and e_W) and "velocity loop" (in e_V) are independent except for these terms. State feedback gains $p, s,$ and c have not yet been determined. The next section derives separate controls for the two loops that guarantee robust performance.

IV. Control Schemes

This section develops control laws for the tension and velocity loops. These schemes are robust in the sense that performance is guaranteed so long as the motor constants $K_{ti} \in [K_{ti_{min}}, K_{ti_{max}}]$ and $\beta_i \in [\beta_{i_{min}}, \beta_{i_{max}}]$, and the unknown damping trajectory $D(\cdot) \in \mathcal{D}$.

A. Velocity Loop—Linear Control

The state equation for the velocity loop can be written

$$\dot{e}_V = (s+c)e_V + u_{b1} - \frac{1}{2}[1 \;\; 1]\mathbf{N}^{-1}(\mathbf{y})\left(\tilde{\mathbf{N}}(\mathbf{y})\mathbf{R}\mathbf{u}_b + \Delta\right). \tag{16}$$

Suppose that $\mathbf{u}_b$ is selected such that

$$\text{sign}\left\{u_{b1} - \frac{1}{2}[1 \;\; 1]\mathbf{N}^{-1}(\mathbf{y})\left(\tilde{\mathbf{N}}(\mathbf{y})\mathbf{R}\mathbf{u}_b + \Delta\right)\right\} = -\text{sign}\{e_V\} \tag{17}$$

for any $K_{ti} \in [K_{ti_{min}}, K_{ti_{max}}]$ and $\beta_i \in [\beta_{i_{min}}, \beta_{i_{max}}]$. Such a $\mathbf{u}_b$ will be calculated below in (40). Then intuitively u_{b1} acts to decrease the magnitude of e_V at least as strongly as the error terms $\frac{1}{2}[1 \;\; 1]\mathbf{N}^{-1}(\mathbf{y})\left(\tilde{\mathbf{N}}(\mathbf{y})\mathbf{R}\mathbf{u}_b + \Delta\right)$ can act

to increase it, so that velocity error goes exponentially fast to zero. The result below puts this in rigorous terms.

Result 1: If $K_{ti} \in [K_{ti_{min}}, K_{ti_{max}}]$, $\beta_i \in [\beta_{i_{min}}, \beta_{i_{max}}]$, and $\mathbf{u}_b$ satisfies (17) with $(s+c)$ a constant, then for any trajectory $e_V(t),\ t \in [t_0, \infty)$, of the system (16)

$$|e_V(t)| \leq |e_V(t_0)| e^{(s+c)(t-t_0)},\ t \geq t_0. \tag{18}$$

Proof: Consider $\xi(t) \equiv e_V^2(t)$. Equation (17) implies $\dot{\xi}(t) \leq 2(s+c)\xi(t)$. By the Comparison Lemma ([4], p. 85), $\xi(t) \leq \xi(t_0) e^{2(s+c)(t-t_0)}$ and therefore $|e_V(t)| \leq |e_V(t_0)| e^{(s+c)(t-t_0)}, \forall t \geq t_0$. ■

This result is independent of air entrainment because $D(\cdot)$ does not appear in (16). The time constant can be arbitrarily selected by choosing the sum $(s+c)$. Because $(s+c)$ is constant, this will be referred to as the "linear velocity loop controller." In practice, making the magnitude of $(s+c)$ too large may cause the inputs to exceed the allowable current level of the DC motors or some other practical limit.

B. Velocity Loop—Nonlinear Control

A constant $(s+c)$ was chosen above for simplicity. However, nonlinear velocity feedback provides much higher performance. Let the feedback gain $(s+c)$ vary in time as a nonlinear function $\{s+c\}(e_V)$ of the velocity error e_V. With $\mathbf{u}_b$ again chosen as in (40), consider the feedback control law

$$\{s+c\}(e_V) \equiv \begin{cases} \frac{-C_1}{|e_V|} & \text{if} \quad |e_V| > C_2 \\ \frac{-C_1}{C_2} & \text{if} \quad |e_V| \leq C_2 \end{cases}, \tag{19}$$

where C_1 and C_2 are positive constants. This scheme applies bang-bang control with maximum value C_1 outside of a small "linear" region defined by C_2. This limits control authority when velocity is far from its target level, but uses more of the available authority when velocity error is smaller.

The small linear region is included to avoid chattering phenomena. Result 1 applies in this linear region, with

$$|e_V(t)| \leq |e_V(t_0)|\, e^{-\frac{C_1}{C_2}(t-t_0)},\ \ \forall t \geq t_0. \tag{20}$$

Performance in the bang-bang range is analytically demonstrated by the following result, which shows that the settling time to the linear region from an initial value $e_V(t_1)$ is less than or equal to $|e_V(t_1)|/C_1$.

Result 2: If $K_{ti} \in [K_{ti_{min}}, K_{ti_{max}}]$, $\beta_i \in [\beta_{i_{min}}, \beta_{i_{max}}]$, and $\mathbf{u}_b$ satisfies (17) then any trajectory $e_V(t),\ t \in [t_0, \infty)$, of the system (16) under the nonlinear control (19), $\exists t_1 \in [t_0, t_0 + |e_V(t_0)|/C_1]$ such that $|e_V(t_1)| \leq C_2$.

Proof: Suppose not, and suppose $e_V(t_0) \geq 0$. (The case where $e_V(t_0) \leq 0$ is analogous.) Then $e_V(t) > C_2$ and $(s+c) = -C_1/|e_V(t)|, \forall t \in [t_0, t_0 + |e_V(t_0)|/C_1]$. Equation (17) implies $\dot{e}_V(t) \leq -C_1$, and by the Comparison Lemma ([4], p. 85) $e_V(t) \leq e_V(t_0) - C_1(t-t_0), \forall t \in [t_0, t_0 + |e_V(t_0)|/C_1]$. Therefore $e_V(t_0 + |e_V(t_0)|/C_1) \leq 0 \leq C_2$, which contradicts $e_V(t_0 + |e_V(t_0)|/C_1) > C_2$. ■

This result is again independent of $D(\cdot)$. Simulations in Section V show how this modified control simultaneously reduces peak motor currents and velocity settling time.

C. Tension Loop

For notational simplicity let $h \equiv c - s$, and note that h can be chosen independently of $(c+s)$. State equations for the tension loop may be rewritten as

$$\begin{aligned} \begin{bmatrix} \dot{e}_T \\ \dot{e}_W \end{bmatrix} &= \begin{bmatrix} 2D(t)p & 2D(t)(h-\sigma) \\ -p & -h \end{bmatrix} \begin{bmatrix} e_T \\ e_W \end{bmatrix} \\ &+ \begin{bmatrix} 2D(t) \\ -1 \end{bmatrix} \left(u_{b2} + \begin{bmatrix} \frac{1}{2} & \frac{-1}{2} \end{bmatrix} \mathbf{N}^{-1}(\mathbf{y}) \left(\tilde{\mathbf{N}}(\mathbf{y}) \mathbf{R} \mathbf{u}_b + \Delta \right) \right) \\ &+ \begin{bmatrix} \frac{\dot{D}(t)}{D(t)}(e_T + T_d) \\ 0 \end{bmatrix}. \end{aligned} \tag{21}$$

Performance is more complicated to analyze for this system because it has two states. Result 3 below uses a Lyapunov function candidate to show that if the feedback gains satisfy

$$\begin{aligned} p &< -\dot{D}_{max}/4D_{min}^2, \\ -\frac{4D_{min}^2 p + \dot{D}_{max}}{2D_{min}} &\leq h \leq \sigma, \end{aligned} \tag{22}$$

with $K_{ti} \in [K_{ti_{min}}, K_{ti_{max}}]$, $\beta_i \in [\beta_{i_{min}}, \beta_{i_{max}}]$, $D(\cdot) \in \mathcal{D}$, and if $\mathbf{u}_b$ is chosen such that

$$\begin{aligned} \text{sign} \left\{ u_{b2} + \frac{1}{2}[1 \quad -1] \mathbf{N}^{-1}(\mathbf{y}) \left(\tilde{\mathbf{N}}(\mathbf{y}) \mathbf{R} \mathbf{u}_b + \Delta \right) \right\} \\ = -\text{sign} \left\{ e_T - e_W \frac{h - \sigma}{p} \right\}, \end{aligned} \tag{23}$$

then

$$|e_T(t)| \leq -\frac{2T_d \dot{D}_{max}}{4D_{min}^2 p + \dot{D}_{max}} \sqrt{\frac{D_{max}}{D_{min}}},\quad \forall t \geq t_0, \tag{24}$$

so long as $e_T(t_0)$ and $e_W(t_0)$ are small enough. For instance, in the common case where $e_W(t_0) = 0$, (24) holds if

$$|e_T(t_0)| \leq -\frac{2T_d \dot{D}_{max}}{4D_{min}^2 p + \dot{D}_{max}} \sqrt{\frac{D(t_0)}{D_{min}}}. \tag{25}$$

Result 3: For the system (21), with (22), (23), $K_{ti} \in [K_{ti_{min}}, K_{ti_{max}}]$, $\beta_i \in [\beta_{i_{min}}, \beta_{i_{max}}]$, and $D(\cdot) \in \mathcal{D}$, if

$$\frac{e_T^2(t_0)}{D(t_0)} + \frac{2(h-\sigma)}{p} e_W^2(t_0) \leq \mathcal{V}_0^2 \tag{26}$$

where

$$\mathcal{V}_0^2 \equiv \frac{4\dot{D}_{max}^2 T_d^2}{D_{min} \left(4D_{min}^2 p + \dot{D}_{max} \right)^2},$$

then any error trajectory $e_T(t),\ t \in [t_0, \infty)$, satisfies (24).

Proof: Consider the function

$$\mathcal{V}(t) \equiv \frac{e_T^2(t)}{D(t)} + \frac{2(h-\sigma)}{p} e_W^2(t), \tag{27}$$

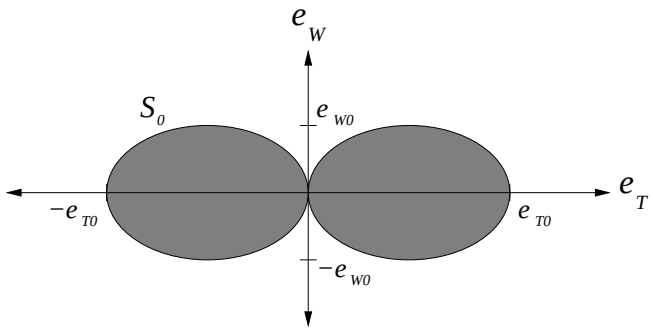

Fig. 2. Phase plane for tension loop.

which is positive definite if $h < \sigma$ and $p < 0$. Then

$$\dot{\mathcal{V}} = \mathcal{U} + 2\left(e_T - \frac{(h-\sigma)e_W}{p}\right) \times \left(2u_{b2} - [-1 \;\; 1]\mathbf{N}^{-1}(\mathbf{y})\left(\tilde{\mathbf{N}}(\mathbf{y})\mathbf{R}\mathbf{u}_b + \Delta\right)\right) \tag{28}$$

with

$$\mathcal{U}(t) \;=\; \left(4p + \frac{\dot{D}(t)}{D^2(t)}\right)e_T^2(t) - \frac{4h(h-\sigma)}{p}e_W^2(t) + \frac{2T_d\dot{D}(t)}{D^2(t)}e_T(t).$$

Without knowing $D(\cdot)$ one can choose $\mathbf{u}_b$ to satisfy (23), so

$$\dot{\mathcal{V}}(t) \le \mathcal{U}(t). \tag{29}$$

Note that the equation $\mathcal{U}(t) = 0$ defines an ellipse in the (e_T, e_W)-plane, which for any time t is contained in the set

$$\mathcal{S}_0 \equiv \left\{(e_T, e_W) : \left(4p \pm \frac{\dot{D}_{max}}{D_{min}^2}\right)e_T^2 - \frac{4h(h-\sigma)}{p}e_W^2 \pm \frac{2T_d\dot{D}_{max}}{D_{min}^2}e_T \ge 0\right\}. \tag{30}$$

(Figure 2 shows the location of $\mathcal{S}_0$ in the (e_T, e_W)-plane.) For all $(e_T, e_W) \in \mathcal{S}_0$,

$$|e_T| \le e_{T0} \equiv \frac{-2\dot{D}_{max}T_d}{4D_{min}^2 p + \dot{D}_{max}}, \tag{31}$$
$$|e_W| \le e_{W0} \equiv \frac{\dot{D}_{max}T_d}{2D_{min}}\sqrt{\frac{-p}{h(h-\sigma)\left(4D_{min}^2 p + \dot{D}_{max}\right)}}.$$

Note that $\dot{\mathcal{V}}(t) < 0$ outside of $\mathcal{S}_0$. At any time t_1, consider the elliptical set $\mathcal{L}(t_1) \equiv \left\{(e_T, e_W) : \mathcal{V}(t_1) \le \mathcal{V}_0^2\right\}$ and its boundary $\partial\mathcal{L}(t_1) \equiv \left\{(e_T, e_W) : \mathcal{V}(t_1) = \mathcal{V}_0^2\right\}$. It is readily shown that if h satisfies (22) then $\mathcal{S}_0 \subset \mathcal{L}(t), \forall t$. This is done by considering two ellipses that have semi-major axes on the same line and share a left endpoint on that line. (If these ellipses are similar and one has at least twice the length and width of the other then they intersect only at this left endpoint.) Because $\mathcal{S}_0 \subset \mathcal{L}(t)$, $\dot{\mathcal{V}}(t) \le 0$ on $\partial\mathcal{L}(t)$. Thus, if $\mathcal{V}(t_0) \le \mathcal{V}_0^2$ then $\mathcal{V}(t) \le \mathcal{V}_0^2$, $\forall t \ge t_0$, and (24) holds. ■

The constraint (23) is analogous to (17), except that here the sign function ensures that $\mathbf{u}_b$ acts to decrease a particular Lyapunov function candidate (rather than a particular state) more than the error terms can act to increase it. The constraints (22) ensure positive-definiteness and other properties of the Lyapunov function candidate, which allows the construction of an invariant set in the (e_T, e_W)-plane. The size of this set determines the bound (24), and can be reduced by choosing p to be more negative, provided an h satisfying (22) exists. In practice, $-p$ cannot be made arbitrarily large because of limits on control authority (such as motor current limits). The bound (24) can also be made smaller by slewing the velocity less aggressively, which reduces $\dot{D}_{max}$.

The system simplifies in steady-state where $\dot{D} \equiv 0$. Result 4 shows that in this case, any trajectory $[e_T(t) \;\; e_W(t)]^\top$ converges exponentially to $[0\;0]$ if (22) and (23) hold.

Result 4: If $K_{ti} \in [K_{ti_{min}}, K_{ti_{max}}]$, $\beta_i \in [\beta_{i_{min}}, \beta_{i_{max}}]$, $\dot{D}(t) \equiv 0$, and (22) and (23) hold then any state trajectory $[e_T(t)\; e_W(t)]^\top$, $t \in [t_0, \infty)$, of the system (21) satisfies

$$\begin{bmatrix} e_T^2(t) \\ e_W^2(t) \end{bmatrix} \le \begin{bmatrix} D \\ \frac{p}{2(h-\sigma)} \end{bmatrix}\left(\frac{e_T^2(t_0)}{D} + \frac{2(h-\sigma)}{p}e_W^2(t_0)\right) \times e^{4D_{min}p(t-t_0)},\; t \ge t_0. \tag{32}$$

Proof: Consider the function

$$\xi(t) \equiv \frac{e_T^2(t)}{D} + \frac{2(h-\sigma)}{p}e_W^2(t). \tag{33}$$

Following (27)-(29),

$$\dot{\xi}(t) \le 4pe_T^2(t) - \frac{4h(h-\sigma)}{p}e_W^2(t), \tag{34}$$

Now

$$\dot{\xi}(t) \le 4D_{min}p\xi(t) + 4p\left(1 - \frac{D_{min}}{D}\right)e_T^2(t) - \frac{2(h-\sigma)}{p}\left(2h + 4D_{min}p\right)e_W^2(t) \tag{35}$$

and hence $\dot{\xi}(t) \le 4D_{min}p\xi(t)$ because $D_{min} \le D$ and $2h + 4D_{min}p \ge 0$ by (22). Then by the Comparison Lemma ([4], p. 85), $\xi(t) \le \xi(0)e^{4D_{min}p(t-t_0)}, t \in [t_0, t_1]$. Then (32) holds since $e_T^2(t) \le D\xi(t)$ and $e_W^2(t) \le p\xi(t)/2(h-\sigma)$. ■

D. Selection of $\mathbf{u}_b$

Results 1-4 hold if $\mathbf{u_b}$ satisfies (17) and (23). These constraints can be written together as

$$\mathbf{u}_b - \frac{1}{2}\mathbf{R}^\top\mathbf{N}^{-1}(\mathbf{y})\left(\tilde{\mathbf{N}}(\mathbf{y})\mathbf{R}\mathbf{u}_b + \Delta\right) = \begin{bmatrix} s_V \\ s_T \end{bmatrix}, \tag{36}$$

where the slack variables s_V and s_T may be any numbers with the desired sign. Using

$$\tilde{\mathbf{N}}(\mathbf{y}) = -\mathbf{N}(\mathbf{y})\begin{bmatrix} \frac{\tilde{K}_{t1}}{K_{t1}} & 0 \\ 0 & \frac{\tilde{K}_{t2}}{K_{t2}} \end{bmatrix}, \tag{37}$$

this readily simplifies to

$$\begin{bmatrix} 2+\frac{\tilde{K}_{t2}}{\hat{K}_{t2}}+\frac{\tilde{K}_{t1}}{\hat{K}_{t1}} & \frac{\tilde{K}_{t2}}{\hat{K}_{t2}}-\frac{\tilde{K}_{t1}}{\hat{K}_{t1}} \\ \frac{\tilde{K}_{t2}}{\hat{K}_{t2}}-\frac{\tilde{K}_{t1}}{\hat{K}_{t1}} & 2+\frac{\tilde{K}_{t2}}{\hat{K}_{t2}}+\frac{\tilde{K}_{t1}}{\hat{K}_{t1}} \end{bmatrix} \mathbf{u}_b \qquad (38)$$
$$-\mathbf{R}^\top \mathbf{N}^{-1}(\mathbf{y})\Delta = 2 \begin{bmatrix} s_V \\ s_T \end{bmatrix},$$

where both sides are multiplied by 2 to simplify notation. Now $\mathbf{u}_b$ must be chosen so that (38) holds over all $K_{ti} \in [K_{ti_{min}}, K_{ti_{max}}]$ and $\beta_i \in [\beta_{i_{min}}, \beta_{i_{max}}]$. Using (37),

$$|\mathbf{R}^\top \mathbf{N}^{-1}(\mathbf{y})\Delta| \le \begin{bmatrix} 1 \\ 1 \end{bmatrix} \Delta_\star \,, \qquad (39)$$

where

$$\Delta_\star(t) \equiv \frac{(\beta_{1_{max}} - \hat{\beta}_1)|V_1(t)|}{J_1(t)} + \frac{(\beta_{2_{max}} - \hat{\beta}_2)|V_2(t)|}{J_2(t)}$$
$$+ \begin{bmatrix} \frac{K_{t1_{max}} - \hat{K}_{t1}}{\hat{K}_{t1}} & \frac{K_{t2_{max}} - \hat{K}_{t2}}{\hat{K}_{t2}} \end{bmatrix} \left| \hat{\mathbf{u}}_0(t) + \hat{\mathbf{M}}(\mathbf{y})\mathbf{e}_x(t) \right|.$$

The matrix premultiplying $\mathbf{u}_b$ in (38) is diagonal except for the $\tilde{K}_{ti}/\hat{K}_{ti}$. Consider

$$\mathbf{u}_b = \begin{cases} \begin{bmatrix} -1 \\ -1 \end{bmatrix} \frac{\Delta_\star \text{sign}\{e_V\}}{2-2(K_{t2_{max}}-\hat{K}_{t2})/\hat{K}_{t2}}, \\ \qquad \text{sign}\{e_V\} = \text{sign}\left\{ e_T - e_W \frac{h-\sigma}{p} \right\} \\ \begin{bmatrix} -1 \\ +1 \end{bmatrix} \frac{\Delta_\star \text{sign}\{e_V\}}{2-2(K_{t1_{max}}-\hat{K}_{t1})/\hat{K}_{t1}}, \\ \qquad \text{sign}\{e_V\} = -\text{sign}\left\{ e_T - e_W \frac{h-\sigma}{p} \right\} \end{cases} . \qquad (40)$$

Because $|u_{b1}| = |u_{b2}|$, either the $\tilde{K}_{t1}/\hat{K}_{t1}$ or the $\tilde{K}_{t2}/\hat{K}_{t2}$ cancel each other in (38). The first term of (38) then contains a factor of $2 - 2\tilde{K}_{ti}/\hat{K}_{ti}$ for some i. The denominator of $\mathbf{u}_b$ is smaller than $2 - 2\tilde{K}_{ti}/\hat{K}_{ti}$ so this $\mathbf{u}_b$ satisfies (38). It simplifies further if both motors are nominally identical. Note that $\mathbf{u}_b$ is undefined if $(K_{ti_{max}} - \hat{K}_{ti})/\hat{K}_{ti} = 1$, so this control can be calculated for any motor parameter tolerance less than 100%. However, it is clear from (40) that greater motor tolerances increase $|\mathbf{u}_b|$, and may therefore lead to higher peak motor currents.

V. Simulation Results

The developed control laws are simulated using parameters based on the testbed tape system described in [7], which appear in Table 4.1. The motors are nominally identical, so $\hat{K}_{t1} = \hat{K}_{t2}$ and $\hat{\beta}_1 = \hat{\beta}_2$. Unlike in [7], a 1.5 Amp/Volt gain in the motor drivers is removed from the torque constants $\hat{K}_{ti}$ so that the inputs are currents. Suppose that the motor specifications guarantee that the true motor constants K_{ti} and β_i are within $\pm 15\%$ of the nominal values $\hat{K}_{ti}$ and $\hat{\beta}_i$. Desired operating tension is $T_d = 0.28$ N, with an allowable peak tension of 0.56 N, and desired velocity is $V_d = 5$ m/s.

For the baseline controller, feedback gains are selected according to equations (18), (22), and (24). Take $s + c = -26$ so that the 2% settling time of the velocity is less than 150 ms. Next, let $p = -500$ so that absolute tension error never exceeds 0.28 N. Finally, (22) requires $h \equiv c - s \ge 110$. In simulation, choosing $c - s$ greater than this minimum leads to higher performance without a substantial increase of the peak motor currents. Hence, take $c - s = 650$. Then $c = 312$ and $s = -338$. Simulations are performed with each motor constant at the boundary of its specified range:

$$\beta_1 = 0.85\hat{\beta} \qquad \beta_2 = 1.15\hat{\beta}$$
$$K_{t1} = 1.15\hat{K}_t \qquad K_{t2} = 0.85\hat{K}_t.$$

Initial tension is $T(0) = 0.4$ N, for an initial error of 0.12 N. Reasonable damping trajectories $D(t)$ have been chosen.

Figure 3 shows a ramp-up maneuver from 0 m/s to 5 m/s. The initial damping is D_{max}, and it changes at a rate close to $-\dot{D}_{max}$. Velocity settling time is 99 ms. High damping (because the system starts at rest with no air entrainment) causes tension error to quickly drop below 0.03 N. Clearly the bound (24) on tension error is conservative, and higher performance is possible in practice.

The input currents have peak magnitude 12 A, which may

TABLE I

System parameters for feedback control simulations

Parameter	Value
ϵ	10 μm
t_p	1.607×10^3 kg/m^3
t_w	8 mm
K_J	20.2 kg/m^2
$r_1(0)$	21.2 mm
$r_2(0)$	9.75 mm
$J_1(0)$	14.2×10^{-6} Kg m^2
$J_2(0)$	10.35×10^{-6} Kg m^2
$\hat{K}_t$	16.53×10^{-3} N m/Amp
$\hat{\beta}$	0.103×10^{-3} N m s/rad
σ	1000 s^{-1}
D_{min}	0.1 N s/m
D_{max}	2 N s/m
$\dot{D}_{max}$	2 N/m

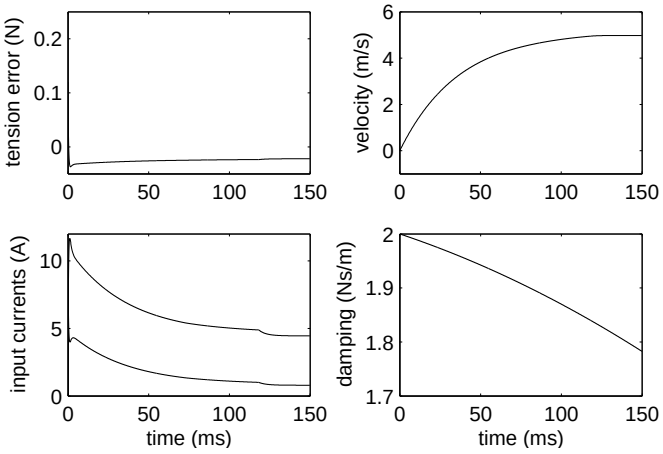

Fig. 3. Velocity ramp-up maneuver.

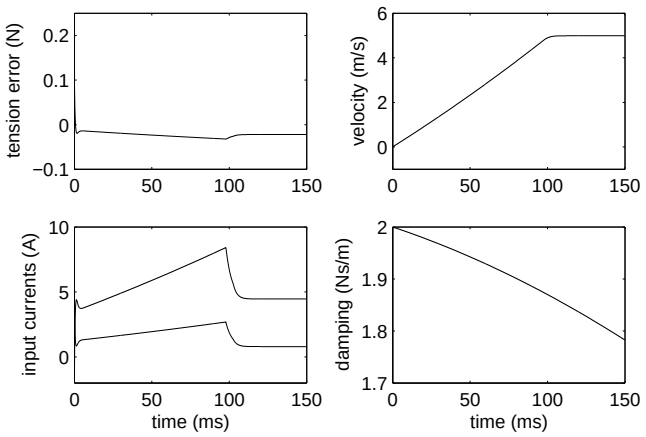

Fig. 4. Velocity ramp-up maneuver—modified controller.

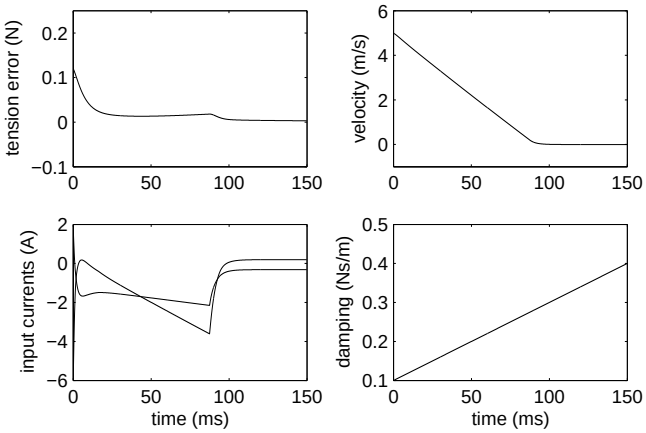

Fig. 5. Velocity ramp-down maneuver—modified controller.

not be feasible in practice. Peak current could be reduced by decreasing the velocity error feedback gain $s + c$, at the expense of increased settling time. However, the modified controller given by (19) reduces both peak currents *and* settling time. Choose $C_1 = 45$, for settling time less than 111 ms to the linear region defined by $C_2 = 0.2$ m/s. For the same desired maneuver, Figure 4 shows the performance of this nonlinear velocity controller. Peak current is a more reasonable 8 A, and settling time is 97 ms. Peak current can be traded for settling time by decreasing C_1, but also varies strongly with the desired robustness to motor parameter errors. Figure 5 shows a ramp-down maneuver, for which tension error drops more slowly because initial damping is much lower. Note that the inputs change slope when the linear region about V_d is reached at 90-100 ms.

Note that the controllers are discontinuous because of the sign$\{\cdot\}$ functions. In practice this may lead to undesirable chattering phenomena. Therefore, these simulations were implemented with sign$\{\cdot\}$ replaced by the approximation

$$\text{sat}_{\epsilon_0}(\tau) = \begin{cases} \text{sign}(\tau) & \text{if} \quad |\tau| \geq \epsilon_0 \\ \frac{\tau}{\epsilon_0} & \text{if} \quad |\tau| < \epsilon_0 \end{cases}, \tag{41}$$

for $\epsilon_0 = 0.1$. Choice of ϵ_0 and the effect of this approximation depend on the size of disturbances in particular systems.

VI. Conclusions and Future Work

This paper presents a nonlinear controller with guaranteed performance. The scheme is robust to air entrainment and uncertainties in the motor torque and friction parameters. Proper choice of feedback gains ensures that velocity error goes exponentially to zero with arbitrary time constant, and tension error remains in a desired range. Tension error is exponentially stable when air entrainment is constant. A modified velocity-loop control provides improved transient response and reduces peak motor currents in simulation. The control law can be calculated for any motor parameter tolerance less than 100%, though peak motor currents may increase with motor parameter tolerance.

Several other disturbances and sources of error might be addressed in the future, such as reel eccentricity and stiction. Further, a control scheme that does not require a tension transducer would allow for significant hardware cost reductions.

VII. References

[1] Baumgart, M. D., and L. Y. Pao, "Transient Control of Web-Winding Systems with Air Entrainment," in *Proc. IFAC Conf. Mechatronic Sys.*, Berkeley, CA, 2002, pp. 17–22.

[2] Franklin, G. F., J. D. Powell, and M. L. Workman, *Digital Control of Dynamic Systems*. Reading, Mass: Addison-Wesley, 1990.

[3] Keshavan, M. B. and J. A. Wickert, "Air Entrainment During Steady-State Web Winding," *ASME J. App. Mech.*, vol. 64, pp. 916–922, 1997.

[4] Khalil, H. K, *Nonlinear Systems*. Upper Saddle River, NJ:Prentice-Hall, 1996.

[5] Lu, Y. and W. C. Messner, "Disturbance Observer Design for Tape Transport Control," in *Proc. Ameri. Ctrl. Conf.*, Arlington, VA, 2001, pp. 2567–2571.

[6] Lu, Y. and W. C. Messner, "Robust Servo Design for Tape Transport," in *Proc. IEEE Intl. Conf. on Ctrl. App.*, Mexico City, Mexico, 2001, pp. 1014–1019.

[7] Mathur, P. D. and W. C. Messner, "Controller Development for a Prototype High-Speed Low-Tension Tape Transport," *IEEE Trans. Ctrl. Sys. Tech.*, vol. 6, no. 4, pp. 534–542, 1998.

[8] Mathur, P. D. and W. C. Messner, "Frequency Domain Characterization of Take-Up Reel Air-Entrainment in Low Tension and High-Speed Tape Transport," *ASME J. Tribology*, vol. 120, pp. 554–558, 1998.

[9] Panda, S. P. and A. P. Engelmann, "Modeling and Control System Design of Reel-to-Reel Tape Drives," in *Proc. Ameri. Ctrl. Conf.*, Anchorage, AK, 2002, pp. 927–932.